Search for TeV Gamma-Rays from the Andromeda Galaxy and for Supersymmetric Dark Matter in the Core of M31

W. Hofmann, D. Horns and H. Lampeitl, for the HEGRA collaboration
Max-Planck-Institut für Kernphysik, D 69029 Heidelberg, P.O. Box 103989

Abstract

Using the HEGRA system of imaging atmospheric Cherenkov telescopes, the Andromeda galaxy (M31) was surveyed for TeV gamma ray emission. Given the large field of view of the HEGRA telescopes, three pointings were sufficient to cover all of M31, including also M32 and NGC205. No indications for point sources of TeV gamma rays were found. Upper limits are given at a level of a few percent of the Crab flux. A specific search for monoenergetic gamma-ray lines from annihilation of supersymmetric dark matter particles accumulating near the center of M31 resulted in flux limits in the 10^{-13} cm^{-2}s^{-1} range, well above the predicted MSSM flux levels except for models with pronounced dark-matter spikes or strongly enhanced annihilation rates.

1. Introduction

M31, as the nearest large galaxy at a distance of 770 kpc, most likely with a black hole of $3 \cdot 10^7$ M$_\odot$ at its core [7], is an obvious target for TeV observations. While conventional sources such as the Crab Nebula would not be visible over the distance to M31, given the current sensitivity of the instruments, the energy output of some of the X-ray sources detected in M31 is at a level which, if continued to higher energy, might be detectable. A particular mechanism for gamma-ray emission is the annihilation of supersymmetric dark matter particles accumulating at the core of M31; rotation curves suggest that M31 contains a significant amount of dark matter.

2. The HEGRA telescope system and the M31 data set

M31 was observed in August, September and November 2001, using all five telescopes of the HEGRA system of Cherenkov telescopes on the Canarian Island of La Palma. Each of the telescopes has a 8.5 m^2 mirror and is equipped with a 271-pixel photomultiplier camera with a 4.3° field of view. The system has an energy threshold around 500 GeV and a 0.1° angular resolution. The detection rate for gamma rays is rather uniform within the central 2° of the field of view, and drops to 63% of its peak value at 1.8° from the optical axis. In order to cover

pp. 1685–1688

all of M31, observation time was distributed between three tracking positions, one centered on the core of M31 at RA 0h 42' 44" DEC 41° 16' 9.12", one displaced by 0.56° to the SW at RA 0h 40' 30" DEC 40° 39' 0" and one displaced to the NE at RA 0h 44' 43" DEC 41° 53' 0". After data cleaning, 20.1 h of good observation time were selected, most of which were taken at Zenith angles below 25°. For calibration and reference, 9.7 h of Crab Nebula data taken in October and November were selected.

In a first analysis step, the entire field was searched for indications of gamma-ray point sources. The data analysis and selection of gamma-ray candidates follows to a large extent the procedures developed for earlier surveys [1,2]. For each grid point, gamma ray candidates with reconstructed directions within 0.143°, consistent within the angular resolution, were counted. Since no specific off-source data were taken, the expected background for each grid point is determined from the data itself, using appropriate background regions in equivalent locations of the field of view of the cameras.

No obvious excess of signal events is visible at any grid point. The significance for each grid point is then calculated based on [8]. The distribution of significances for all grid points approximates a Gaussian distribution with unit width, as expected in the absence of a genuine signal; the point with the highest significance of 3.5 σ is well compatible with the expected tail of the Gaussian distribution, and should be interpreted as an upward fluctuation.

We conclude that there is no statistically significant indication of a TeV gamma ray point source in M31, and extract upper limits for the source flux. The 99% confidence level on the number of excess events is calculated for each grid point, and is converted into a flux using the measured gamma-ray rate from the Crab Nebula. The resulting flux limits are shown in Fig. 1 (left), and range from 3.3% of the Crab flux for the center of M31 to about 30% at the periphery. For two other objects in the survey range, M32 and NGC205, limits of 4.4% and 2.8% of the Crab flux are derived, respectively. More details can be found in [3].

3. Search for supersymmetric dark matter in M31

Beyond the general survey, the good energy resolution of the HEGRA telescope system allows a dedicated search for supersymmetric dark matter in M31, looking for the line emission from the self-annihilation of the lightest stable particle (LSP). We have searched for line emission in the energy spectrum from the central part of M31 ($r < 1.4$ kpc), and compare the results with predictions of the flux of gamma-rays from the annihilation of neutralinos (χ_0) in the framework of the minimal supersymmetric standard model (MSSM) using a spatial distribution of the radial density of neutralinos in M31 in concordance with the measured rotation curve [6].

In order to reduce the background from isotropic cosmic ray events, in the

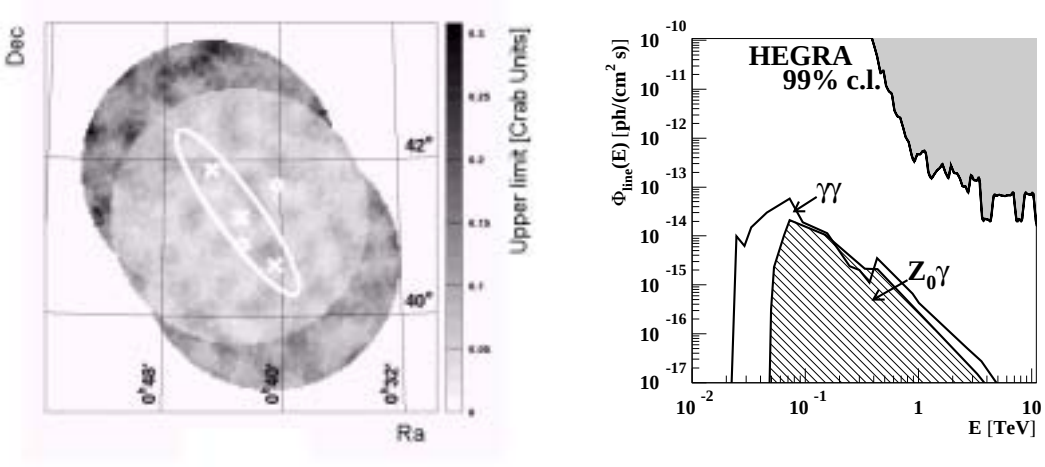

Fig. 1. Left: Upper limits on the flux from TeV point sources in M31, expressed in units of the Crab flux. For reference, the locations of the center of M31, the 10 kpc dust ring and the two companion galaxies M32 and NGC205 are indicated. Tracking positions are indicated by crosses. Right: Exclusion region (grey shaded region) for the the gamma-ray line flux from the center of M31. The two sets of curves labeled $\gamma\gamma$ and $Z^0\gamma$ indicate the upper range of model predictions for the minimal supersymmetric models calculated in [4].

event selection a tight cut on the direction has been chosen for the central part of M31. Only events from within a cone of radius 0.105° are accepted. At a distance of 770 kpc this corresponds to the inner 1.4 kpc of M31. The sensitivity for line emission depends on the energy resolution of the detector. For this analysis, an improved energy reconstruction algorithm has been applied. The relative energy resolution ($\Delta E/E$) reaches 10 % for a wide energy band from the threshold of 500 GeV up to 10 TeV. The search bin in energy is 12 % wide, concentrating on the central section of a monoenergetic line in order to achieve best signal to noise ratios. The energy bins are equally spaced on a logarithmic scale such that the bin centers are separated by 0.025 on a decadic logarithmic scale, making the bins correlated.

The background expectation of the measurement is determined using seven independent OFF-regions with similar acceptance to the ON-region. For the calculation of upper limits on the number of excess events $N_\gamma^{99\,\%}$, the 99 % c.l. upper limits were caculated and an upper limit on the rate from a γ-ray line was derived. The corresponding flux limits were calculated using collection areas $A_{eff}(E,\theta)$ derived from Monte Carlo simulations applying the same reconstruction methods and event selection as for the data analysis. The resulting exclusion region is indicated in Fig. 1 (right) as the grey shaded region.

A prediction for the line flux emission was derived using scans of the 7-

parameter space of MSSM performed by [4]. The expected flux is given by Eq. (6) of [6] or the equivalent Eq. (13) of [4] (scaled to the distance to M31):

$$I_\gamma = (3.18 \cdot 10^{-13} \text{ photons cm}^{-2} \text{ s}^{-1}) \left(\frac{\langle \sigma v \rangle N_\gamma}{10^{-25} \text{ cm}^3 \text{ s}^{-1}} \right) \left(\frac{500 \text{ GeV}}{m_\chi} \right)^2 \Sigma_{19}$$

Apart from trivial factors, it depends on the velocity-weighted annihilation cross section $\langle \sigma v \rangle$ and on the line-of-sight and solid-angle integrated squared LSP mass density ρ

$$\Sigma = \int \int \rho^2 \, \mathrm{d}s \, \mathrm{d}\Omega$$

written as Σ_{19} in units of 10^{19} GeV^2 cm^{-5}. The envelope of the allowed $\langle \sigma v \rangle$ vs. m_χ space was used as given in Figs. 1 and 2 of [4]. The unitless parameter $\Sigma_{19} \approx 1.7$ corresponds to $\Sigma_{19} = 3$ of [6], scaled to the inner 1.4 kpc on the basis of the $\rho(r)$ distributions of Fig. 3(b) of [6] and using a distance of 770 kpc. This value of Σ_{19} represents the upper range of the different models for the dark matter halo of M31 discussed in this reference. The predicted line flux is given in Fig. 2 (right). We have indicated the two individual final states with line emission ($\chi^0\chi^0 \to \gamma\gamma$ and $\chi^0\chi^0 \to Z^0\gamma$) in the figure. The model prediction given here is based upon smoothly distributed dark matter. Within this model, no signal from M31 with the current sensitivity of Cherenkov detectors is to be expected. Very favorable conditions as for example clumpiness of dark matter would lead to a considerable increase of the annihilation rate [5,9]. It is conceivable that the flux level of some models would become detectable by tuning the distribution of the dark matter halo and by invoking mechanisms to allow for larger cross sections. However, in the absence of a signal, no exotic speculations are required.

Acknowledgement

The support of HEGRA by the Spanish CICYT and the German Ministry for Education and Research BMBF is gratefully acknowledged.

1. Aharonian, F.A., Akhperjanian, A.G., Barrio, J.A., et al. 2001, A&A 375, 1008
2. Aharonian, F.A., Akhperjanian, A.G.,Beilicke, M., et al. 2002, A&A 395, 803
3. Aharonian, F.A., Akhperjanian, A.G., Beilicke, M., et al. 2003, A&A 400, 153
4. Bergström, L., Ullio, P., & Buckley, J.H., 1998, Astropart. Phys. 9, 137
5. Bergström, L, Edsjö, J, Gondolo, P, & Ullio, P., 1999, Phys. Rev. D59, 043506
6. Falvard, A., Giraud, E., Jacholkowska, A., et al. 2002, astro-ph/0210184
7. Kormendy, J., & Bender, R., 1999, ApJ 522, 772
8. Li, T., & Ma, Y., 1983, ApJ 272, 317
9. Taylor, J.E., & Silk, J. 2002, submitted to MNRAS, astro-ph/0207299